AIP | The Journal of Chemical Physics

The rotational spectrum of CuCCH(1+): A Fourier transform microwave discharge assisted laser ablation spectroscopy and millimeter/submillimeter study

M. Sun, D. T. Halfen, J. Min, B. Harris, D. J. Clouthier et al.

Citation: J. Chem. Phys. **133**, 174301 (2010); doi: 10.1063/1.3493690
View online: http://dx.doi.org/10.1063/1.3493690
View Table of Contents: http://jcp.aip.org/resource/1/JCPSA6/v133/i17
Published by the American Institute of Physics.

The rotational spectrum of CuCCH($\tilde{X}\ ^1\Sigma^+$): A Fourier transform microwave discharge assisted laser ablation spectroscopy and millimeter/submillimeter study

M. Sun,[1] D. T. Halfen,[1] J. Min,[1] B. Harris,[1] D. J. Clouthier,[2] and L. M. Ziurys[1,a)]
[1]*Department of Chemistry and Department of Astronomy, Arizona Radio Observatory, and Steward Observatory, University of Arizona, Tucson, Arizona 85721, USA*
[2]*Department of Chemistry, University of Kentucky, Lexington, Kentucky 40506, USA*

(Received 28 July 2010; accepted 7 September 2010; published online 1 November 2010)

The pure rotational spectrum of CuCCH in its ground electronic state ($\tilde{X}\ ^1\Sigma^+$) has been measured in the frequency range of 7–305 GHz using Fourier transform microwave (FTMW) and direct absorption millimeter/submillimeter methods. This work is the first spectroscopic study of CuCCH, a model system for copper acetylides. The molecule was synthesized using a new technique, discharge assisted laser ablation spectroscopy (DALAS). Four to five rotational transitions were measured for this species in six isotopologues (^{63}CuCCH, ^{65}CuCCH, ^{63}Cu^{13}CCH, ^{63}CuC^{13}CH, ^{63}Cu^{13}C^{13}CH, and ^{63}CuCCD); hyperfine interactions arising from the copper nucleus were resolved, as well as smaller splittings in CuCCD due to deuterium quadrupole coupling. Five rotational transitions were also recorded in the millimeter region for ^{63}CuCCH and ^{65}CuCCH, using a Broida oven source. The combined FTMW and millimeter spectra were analyzed with an effective Hamiltonian, and rotational, electric quadrupole (Cu and D) and copper nuclear spin-rotation constants were determined. From the rotational constants, an $r_m^{(2)}$ structure for CuCCH was established, with $r_{Cu—C}=1.8177(6)$ Å, $r_{C—C}=1.2174(6)$ Å, and $r_{C—H}=1.046(2)$ Å. The geometry suggests that CuCCH is primarily a covalent species with the copper atom singly bonded to the C≡C—H moiety. The copper quadrupole constant indicates that the bonding orbital of this atom may be *sp* hybridized. The DALAS technique promises to be fruitful in the study of other small, metal-containing molecules of chemical interest. © *2010 American Institute of Physics*.
[doi:10.1063/1.3493690]

I. INTRODUCTION

Organocopper reagents have widespread usage in organic chemistry.[1] These compounds have many desirable synthetic properties as alkylating agents, including regioselectivity in carbon-carbon bond formation.[2] For instance, the Gilman reagent (lithium alkyl cuprate: R_2CuLi) is particularly useful for conjugate or 1,4-addition to α,β-unsaturated aldehydes and ketones.[3,4] In the Ullmann reaction, biaryls are created through an active copper(I)-compound, which undergoes oxidative addition followed by reductive elimination, resulting in formation of an aryl-aryl carbon bond.[5,6]

The use of copper acetylides (CuC≡CR, R=H, CH_3, C_6H_5, etc.) in organic synthesis began in 1859, when Böttger created the first organocopper compound, dicopper(I) acetylide (CuC≡CCu).[7] Despite the fact that this species and other similar small organocopper acetylides are explosive in air,[3,4,8] they are useful reagents in solution. Substitution reactions with copper acetylides (Castro–Stephens couplings) have long been known to be a convenient route to a wide variety of aromatic acetylides.[9] Allylic and aryl halides also react with copper acetylide reagents to form indoles, benzofurans, phthalides, thianaphthenes, and furans.[10] These copper species can also be found as active intermediates in organic transformations, such as in the Cadiot–Chodkiewicz reaction.[11,12] Here a terminal alkyne and a haloalkyne are coupled together via a copper acetylide intermediate, offering access to asymmetrical dialkynes. Another widely used process is the Sonogashira reaction, which couples terminal alkynes with aryl halides, alkyl halides, vinyl halides, arynes, azides, and allylic ethers in the presence of a palladium catalyst and a copper (I) cocatalyst.[3,13–17] Evidence has been found for *in situ* formation of copper acetylides as a key step in the overall process, which then proceeds through Pd—Cu transmetalation.[18] However, the role of the copper catalyst cycle is still poorly understood.[19] Dicopper(I) acetylide has also been used to make nanowires and nanocables,[8] and solid state material with carbyne moieties.[20]

Despite their widespread use in synthesis, little is known about the fundamental properties of individual copper acetylide species, perhaps because of their explosive, as well as elusive, chemical behavior. The need for spectroscopic characterization of simple copper acetylides would seem to be imperative in order to understand their catalytic and synthetic functions. Yet, spectroscopic investigation of copper acetylides has been limited to solid-state infrared and Raman measurements of the vibrational frequencies of copper methylacetylide ($CuC{\equiv}CCH_3$), copper butylacetylide ($CuC{\equiv}C(CH_2)_3CH_3$), and copper phenylacetylide

a)Electronic mail: lziurys@as.arizona.edu.

($CuC{\equiv}CC_6H_5$).[21] The simplest copper acetylide, CuCCH, has never been studied by any spectroscopic method, although it is clearly the model system for this class of compounds.

In this paper, we present the first spectroscopic study of copper monoacetylide, CuCCH. The pure rotational spectrum of this molecule in its $\tilde{X}\ ^1\Sigma^+$ ground electronic state was recorded using a combination of Fourier transform microwave (FTMW) and millimeter/submillimeter direct absorption methods across the 7–305 GHz frequency range. Copper hyperfine interactions were resolved in the FTMW data. In order to create CuCCH, a new technique was developed for the FTMW instrument: discharge assisted laser ablation spectroscopy (DALAS). This method facilitated the study of six isotopologues of this species, which has enabled an accurate structure determination. Here we describe our measurements and analysis of CuCCH, and discuss some implications for copper metal-ligand bonding.

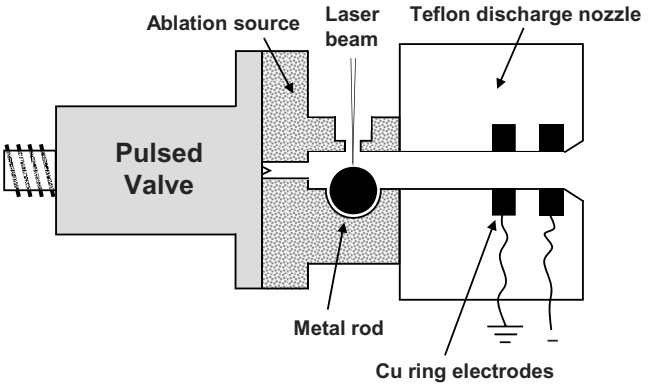

FIG. 1. A diagram of the DALAS source. The device consists of a conventional supersonic nozzle/laser ablation apparatus, modified by the addition of a pulsed dc discharge nozzle. A miniature motor translates and rotates the metal rod, which is ablated through a small opening (2–3 mm in diameter) by a laser (Nd:YAG) beam. The dc discharge source consists of two copper ring electrodes in a Teflon housing with a 5 mm diameter flow channel flared at a 30° angle at the exit.

II. EXPERIMENTAL

Prior to the search for the spectrum of CuCCH, density functional theory was used to calculate the ground state properties using the GAUSSIAN 03 program suite.[22] The *Becke* three parameter hybrid density functional with the *Lee*, *Yang*, and *Parr* correlation functional (B3LYP) was employed with *Dunning*'s correlation consistent triple-zeta basis set augmented by diffuse functions (aug-cc-pVTZ) to predict the geometry, vibrational frequencies, rotational constant, and copper quadrupole coupling constant.[23–25] A stable stationary point with a linear copper acetylide geometry was found on the CuCCH potential energy surface with a dipole moment of 3.6 D, indicating the feasibility of microwave studies.

Measurements of the pure rotational spectrum of CuCCH were then conducted using the Balle–Flygare-type Fourier transform microwave (FTMW) spectrometer of Ziurys and co-workers.[26,27] This instrument consists of a vacuum chamber (unloaded pressure about 10^{-8} Torr maintained by a cryopump), which contains a Fabry–Pérot cavity consisting of two spherical aluminum mirrors in a near confocal arrangement. Antennas are embedded in the mirrors for the injection and detection of microwave radiation. A supersonic jet is introduced into the cavity by a pulsed valve (General Valve, 0.8 mm nozzle orifice), aligned 40° relative to the optical axis. Time domain signals are recorded over a 600 kHz frequency range from which spectra with 2 kHz resolution are created via a fast Fourier transform. Transitions appear as Doppler doublets with a full width at half maximum of 5 kHz; transition frequencies are taken as the doublet average. More details regarding the instrumentation can be found in Ref. 27.

To initially create CuCCH, DALAS was used. DALAS is a new technique for creating metal-bearing species. The DALAS apparatus consists of a Teflon dc discharge nozzle attached to the end of a pulsed-nozzle laser ablation source, as shown in Fig. 1. The laser ablation mechanism bolts to the pulsed valve (General Valve) and contains a 2.5–5 mm wide channel for the gas flow. A 6 mm diameter rod composed of the metal of interest, which is attached to a motorized actuator (MicroMo 1516 SR) for translation and rotation, slides into the ablation housing. The housing contains a 2–3 mm diameter hole to allow the ablating laser beam to intersect the rod. The dc discharge source, consisting of two copper ring electrodes in a Teflon housing, has a 5 mm diameter channel for exiting gas, which is flared at the end with a 30° angle. To accommodate the angled nozzle source, the laser beam enters the vacuum chamber at a 50° angle relative to the mirror axis through a borosilicate window. A "docking station" was attached to the laser window to ensure perpendicular alignment of the metal rod relative to the laser beam. The second harmonic (532 nm) of Nd:YAG (yttrium aluminum garnet) laser (Continuum Surelite I-10) is used for the ablation. The DALAS source was operated at a rate of 10 Hz.

CuCCH was produced in the DALAS source from a mixture of 0.1% acetylene in argon and the ablation of a copper rod (ESPI Metals). The gas pulse, which is 550 μs in duration, was introduced into the chamber at a stagnation pressure of 310 kPa (absolute). The laser, set at a flash-lamp voltage of 1.20 kV (200 mJ/pulse), was fired 990 μs after the initial opening of the valve. The dc discharge, using a voltage of 0.8 kV at 30 mA, was turned on for 1390 μs following the triggering of the valve pulse. The spectra of ^{63}CuCCH and ^{65}CuCCH were obtained in their natural abundance, while for the ^{13}C and D isotopologues of CuCCH, 0.1% DCCD (Cambridge Isotopes, 99% enrichment) or 0.2% $^{13}CH_4$ (Cambridge Isotopes, 99% enrichment) were used, respectively. A mixture of 0.1% CH_4 and 0.1% $^{13}CH_4$ was employed for Cu^{13}CCH and Cu^{13}CCH. Typically, 250–500 pulses were accumulated to achieve an adequate signal-to-noise ratio for the main isotopologue, while for the other species, 250–2000 pulses were necessary.

Once the identity of CuCCH was confirmed, the millimeter/submillimeter spectrum was recorded using one of the direct absorption spectrometers of Ziurys *et al.*[28] Briefly, the instrument consists of a radiation source, gas cell, and detector. The frequency source is a series of Gunn oscillator/Schottky diode multiplier combinations that cover

the range of 65–850 GHz. The reaction chamber is a double-pass steel cell, which contains a Broida-type oven. The detector is a liquid helium-cooled hot electron bolometer. The radiation passes quasioptically from a scalar feedhorn through the system via a series of Teflon lenses, a rooftop reflector, and a polarizing grid, and into the detector. Frequency modulation of the Gunn oscillator at a rate of 25 kHz is employed for phase-sensitive ($2f$) detection, and a second-derivative spectrum is obtained.

For the millimeter measurements, CuCCH was synthesized in a dc discharge by the reaction of copper vapor, produced in the Broida oven, with acetylene in argon carrier gas. The best signals were obtained using 5–10 mTorr of HCCH, introduced over the oven, and 10 mTorr of Ar, flowed from underneath the oven, with a discharge of 1 A at 50 V. About 10 mTorr of argon was also continuously streamed over the cell lenses to help prevent coating by the metal vapor. The plasma exhibited a dark green color due to atomic emission from copper.

Transition frequencies were measured by averaging pairs of 5 MHz wide scans, one scan increasing in frequency, and the other decreasing in frequency. One to five scan pairs were needed to achieve a sufficient signal-to-noise ratio. The center frequency and line width were determined by fitting the line profile with a Gaussian function. The line widths varied from 630 to 750 kHz in the frequency range of 261–305 GHz. The experimental accuracy is estimated to be ± 50 kHz.

III. RESULTS

Based on the theoretical calculations, the $J=2\rightarrow 1$ transition of CuCCH was searched for using the DALAS technique with the FTMW instrument near 16 GHz. Searches for this molecule had previously been conducted at millimeter wavelengths, and also with the FTMW machine with a laser ablation source, but without success. Using DALAS, two clusters of lines were found near 16.28 and 16.48 GHz, both due to a copper-containing species. The patterns were similar, with a relative intensity ratio of about 2:1, and resembled the predicted splittings for copper quadrupole interactions. $[I(^{63}\mathrm{Cu})=I(^{65}\mathrm{Cu})=3/2]$.[29] Transitions at higher and lower frequencies were then observed for both sets of lines, leading to the unambiguous assignment of ^{63}CuCCH and ^{65}CuCCH ($^{63}\mathrm{Cu}:^{65}\mathrm{Cu}=69:31$).[29] Following these measurements, the spectra of $^{63}\mathrm{Cu}^{13}\mathrm{C}^{13}\mathrm{CH}$, $^{63}\mathrm{Cu}^{13}\mathrm{CCH}$, $^{63}\mathrm{CuC}^{13}\mathrm{CH}$, and CuCCD were recorded with the FTMW instrument, spanning the range of 7.5–39.5 GHz.

As shown in Table I, 23 and 17 individual copper hyperfine components were measured in the range of 8–33 GHz for ^{63}CuCCH and ^{65}CuCCH, respectively, arising from the four rotational transitions $J=1\rightarrow 0$ through $J=4\rightarrow 3$. For both $^{63}\mathrm{Cu}^{13}\mathrm{C}^{13}\mathrm{CH}$ and $^{63}\mathrm{Cu}^{13}\mathrm{CCH}$, 17 hyperfine lines were recorded, and 21 for $^{63}\mathrm{CuC}^{13}\mathrm{CH}$, all originating in the $J=1\rightarrow 0$ through $J=4\rightarrow 3$ or $J=5\rightarrow 4$ transitions (see Table I). Hyperfine interactions from the ^{13}C nuclear spin of $I=1/2$ were not observed for any of these isotopologues. For ^{63}CuCCD, hyperfine splittings due to the deuterium nucleus ($I=1$) were resolved, as well as those from copper, and a total of 88 lines were recorded from five rotational transitions; these data are available electronically.[30]

Also shown in Table I are the millimeter/submillimeter rotational transitions recorded for ^{63}CuCCH and ^{65}CuCCH. Five rotational transitions were measured for each isotopologue in the frequency range of 261 to 305 GHz. At these frequencies, the quadrupole structure found at lower J is completely collapsed, and the transitions appear as single lines.

Representative spectra of CuCCH measured with the FTMW instrument are displayed in Figs. 2 and 3. In Fig. 2, the $J=1\rightarrow 0$ transition of the main isotopologue, ^{63}CuCCH, near 8.2 GHz is shown. This transition consists of several hyperfine components arising from the ^{63}Cu nuclear spin, indicated by the quantum number F. The Doppler doublets for each feature are indicated by brackets. The $J=1\rightarrow 0$ spectrum shows the classic triplet quadrupole pattern; there are two frequency breaks in these data to display all three features. The spectrum of $^{63}\mathrm{Cu}^{13}\mathrm{C}^{13}\mathrm{CH}$ exhibits a similar pattern to the main isotopologue, but with somewhat weaker signal strength because of less efficient chemical production. For the ^{13}C singly substituted species, the hyperfine patterns are the same as for ^{63}CuCCH, as the ^{13}C hyperfine structure was again not resolved.

In Fig. 3, the $J=2\rightarrow 1$ transition of ^{63}CuCCD at 15 GHz is shown. Although the hyperfine interactions arising from ^{63}Cu are dominant, indicated by quantum number F_1, splittings due to deuterium are also resolved in this species, labeled by F $[F=F_1+I(\mathrm{D})]$. The splittings arising from the deuterium nucleus are comparable in magnitude to the Doppler doubling.

Representative millimeter-wave spectra are shown in Fig. 4. Here the $J=35\leftarrow 34$ transition of ^{63}CuCCH (upper panel) and ^{65}CuCCH (lower panel) near 288 and 286 GHz, respectively, are presented. The data are displayed on the same intensity scale to illustrate the observed natural abundance ratio of $^{63}\mathrm{Cu}/^{65}\mathrm{Cu}\sim 2/1$.[29]

IV. ANALYSIS

The spectra of the six CuCCH isotopologues were individually analyzed using an effective $^1\Sigma$ Hamiltonian consisting of rotation, electric quadrupole coupling, and nuclear spin-rotation terms[31]

$$H_{\mathrm{eff}}=H_{\mathrm{rot}}+H_{eQq}+H_{\mathrm{nsr}}. \quad (1)$$

A combined fit of the FTMW and millimeter measurements, weighted by the experimental accuracies, was carried out in cases where both data sets were available, i.e., ^{63}CuCCH and ^{65}CuCCH. The nonlinear least-squares routine SPFIT was employed to analyze the data and obtain spectroscopic parameters,[32] and the results are given in Table II. In addition to the rotational parameters B and D, the electric quadrupole coupling constant eQq was determined for the copper nuclei in all species, as well as for the deuterium nucleus in ^{63}CuCCD. In contrast, the nuclear spin-rotation parameter C_{I} could only be determined for the ^{63}Cu and ^{65}Cu nuclei; attempting to fit this constant for the either deuterium or ^{13}C resulted in values that were undefined to within their 3σ

TABLE I. Observed rotational transitions (MHz) of CuCCH and its Cu and C isotopologues ($\tilde{X}\ ^1\Sigma^+$).

		^{63}CuCCH		^{65}CuCCH		^{63}CuC^{13}CH		^{63}Cu^{13}CCH		^{63}Cu^{13}C^{13}CH	
$J' \leftrightarrow J''$	$F' \rightarrow F''$	ν_{obs}	$\nu_{obs}-\nu_{calc}$	ν_{obs}	$\nu_{obs}-\nu_{calc}$	ν_{obs}	$\nu_{obs}-\nu_{calc}$	ν_{obs}	$\nu_{obs}-\nu_{calc}$	ν_{obs}	$\nu_{obs}-\nu_{calc}$
1→0	0.5→1.5	8237.454	0.002	8172.466	0.001	7892.589	0.000	8155.981	0.000	7821.166	0.000
	2.5→1.5	8240.766	0.000	8175.535	0.000	7895.900	−0.002	8159.298	0.000	7824.484	0.002
	1.5→1.5	8244.842	0.000	8179.306	0.001	7899.974	−0.004	8163.375	−0.003	7828.562	−0.001
2→1	1.5→1.5	16 479.819	0.000	16 349.480	0.002	15 790.093	0.000	16 316.880	−0.001	15 647.255	0.002
	2.5→1.5	16 482.765	−0.003	16 352.209	0.000	15 793.039	−0.003	16 319.830	−0.002	15 650.199	−0.005
	3.5→2.5	16 482.778	0.001	16 352.221	0.003	15 793.050	−0.001	16 319.843	0.002	15 650.213	0.001
	0.5→0.5	16 483.097	0.001	16 352.512	0.000	15 793.372	0.001	16 320.161	−0.001	15 650.532	−0.002
	2.5→2.5	16 486.844	0.001	16 355.981	0.002	15 797.120	0.002	16 323.912	0.000	15 654.285	0.000
	1.5→0.5	16 487.209	0.001	16 356.318	0.000	15 797.483	0.000	16 324.279	0.001	15 654.650	0.000
3→2	1.5→1.5	24 721.292	0.000								
	2.5→2.5	24 722.463	0.000								
	3.5→2.5	24 724.407	0.000	24 528.546	0.001	23 689.821	−0.001	24 480.003	−0.001	23 475.565	−0.004
	4.5→3.5	24 724.416	0.000	24 528.558	0.004	23 689.831	0.000	24 480.013	0.000	23 475.578	0.001
	1.5→0.5	24 725.405	0.001	24 529.465	−0.001	23 690.819	−0.001	24 481.001	−0.001	23 476.569	0.002
	2.5→1.5	24 725.413	0.001	24 529.477	0.002	23 690.830	0.002	24 481.014	0.004	23 476.579	0.004
	3.5→3.5	24 728.474	0.001								
4→3	2.5→2.5	32 962.209	0.001								
	3.5→3.5	32 964.393	−0.001								
	4.5→3.5	32 965.872	0.001	32 704.712	−0.003	31 586.434	0.000	32 639.999	−0.002	31 300.766	−0.002
	5.5→4.5	32 965.881	0.000	32 704.723	−0.001	31 586.445	0.002	32 640.008	−0.002	31 300.778	0.001
	2.5→1.5	32 966.325	−0.004	32 705.136	−0.001	31 586.893	0.001	32 640.460	0.001	31 301.226	−0.001
	3.5→2.5	32 966.339	0.001	32 705.141	−0.004	31 586.903	0.002	32 640.470	0.002	31 301.236	0.001
	4.5→4.5	32 969.928	−0.001								
5→4	5.5→4.5					39 482.902	0.000				
	6.5→5.5					39 482.912	0.001				
	3.5→2.5					39 483.162	−0.003				
	4.5→3.5					39 483.173	−0.001				
32←31	[a]	263 568.134	0.008	261 481.199	0.051						
34←33	[a]	280 018.881	−0.018	277 801.810	−0.003						
35←34	[a]	288 242.789	0.004	285 960.662	−0.004						
36←35	[a]	296 465.625	−0.005	294 118.482	−0.012						
37←36	[a]	304 687.414	0.009	302 275.252	−0.016						

[a]Hyperfine collapsed.

uncertainties. The combined FTMW/millimeter-wave analyses give excellent rms values of 4 kHz (^{63}CuCCH) and 12 kHz (^{65}CuCCH); the values for the other isotopologues are 2 kHz, which are typical for FTMW measurements

V. DISCUSSION

A. DALAS: A new molecule production method

Discharge assisted laser ablation spectroscopy (DALAS) was essential for our success in detecting CuCCH by FTMW methods. The spectra of this molecule could not be produced without the simultaneous use of both the laser ablation and the dc discharge sources in our FTMW spectrometer. The ablation source alone did not create CuCCH in detectable quantities. Experiments with other known species, such as ZnO, showed an increase in S/N as high as a factor of 20 when using DALAS, as opposed to laser ablation itself. It was also found that higher laser power (1.20 kV flash lamp voltage) could be employed with DALAS. Without the discharge, the laser flash lamp voltage had to be decreased to 1.08 kV, and molecule production was found to vary more erratically from pulse to pulse. The duration of the dc discharge was also found to be critical, depending on the species. Production of CuCCH, ZnO, and other closed-shell species was optimal when the dc discharge was turned off 300–400 μs after the laser pulse (total length is 1300–1400 μs); for radicals such as MgCCH and ZnCCH, production was better when the discharge duration was reduced to a total time of 1000 μs, i.e., terminated immediately after the laser pulse.

At this time, we can only speculate on the efficacy of the DALAS technique. Initially, we thought that the discharge might be degrading larger clusters produced by ablation, yielding the smaller molecules of interest, although we have no experimental evidence that this is the case. For the specific example of ZnO, the reaction of ground state Zn atoms with O_2 to produce the monoxide is highly endothermic,[33] so it may be that the discharge provides excited state Zn atoms and/or dissociates the O_2 molecules to more reactive oxygen atoms. Also, the extended "on time" of the discharge (1000–1400 μs) compared to the relatively short ablation event (5 ns) may help provide a greater concentration of reactive species. In the case of copper acetylide, previous studies have shown that ground state thermalized copper at-

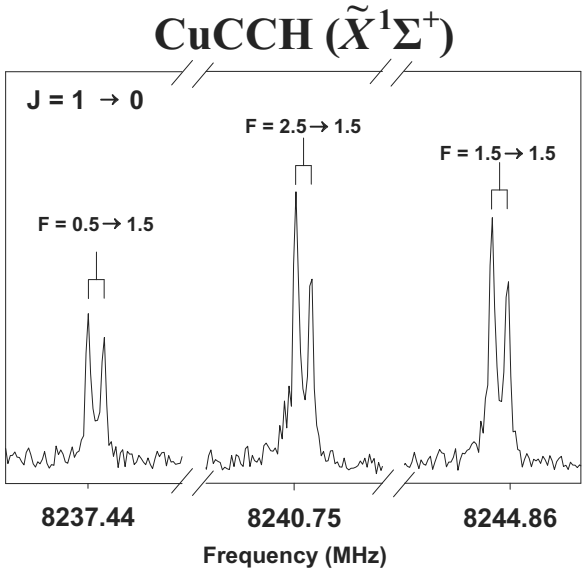

FIG. 2. FTMW spectrum of the $J=1\rightarrow0$ transition of the CuCCH main isotopologue, measured near 8.2 GHz. This transition is composed of hyperfine components due to ^{63}Cu nuclear spin ($I=3/2$), labeled by quantum number F. Doppler doublets are indicated by brackets. There are two frequency breaks in the spectrum in order to show all three hyperfine lines. The spectrum is a compilation of three 300 kHz wide scans with 250 pulse averages per scan.

oms react with acetylene to produce the mono- and diacetylene copper complexes.[34] Thus, it may be necessary to either activate the copper atoms produced by laser ablation to give a greater yield of electronically excited species or to fragment the acetylene reactant to efficiently produce CuCCH. Either mechanism may be an operant in DALAS. It would be of interest to use mass spectrometry or some other analytical technique to further our understanding of the processes involved in hopes of optimizing and improving the method.

An experimental apparatus similar to DALAS has been

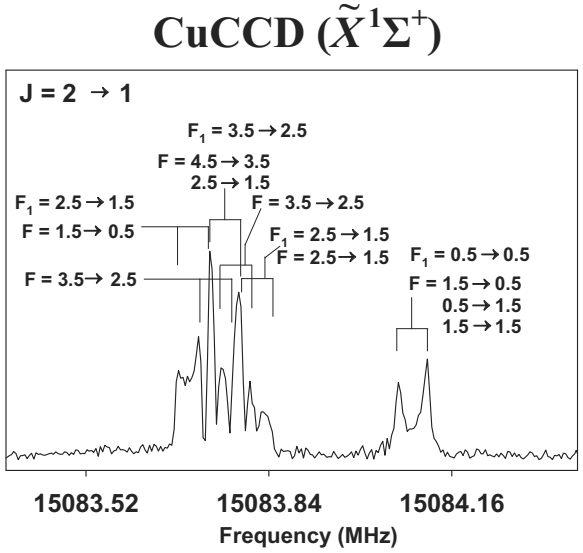

FIG. 3. FTMW spectrum of the $J=2\rightarrow1$ transition of CuCCD near 15 GHz showing the hyperfine interactions originating with the ^{63}Cu nuclear spin, which is indicated by quantum number F_1, as well as the deuterium nucleus ($I=1$) labeled by F. Brackets show the Doppler doublets. This spectrum is a compilation of two 500 kHz wide scans with 1000 pulse averages per scan.

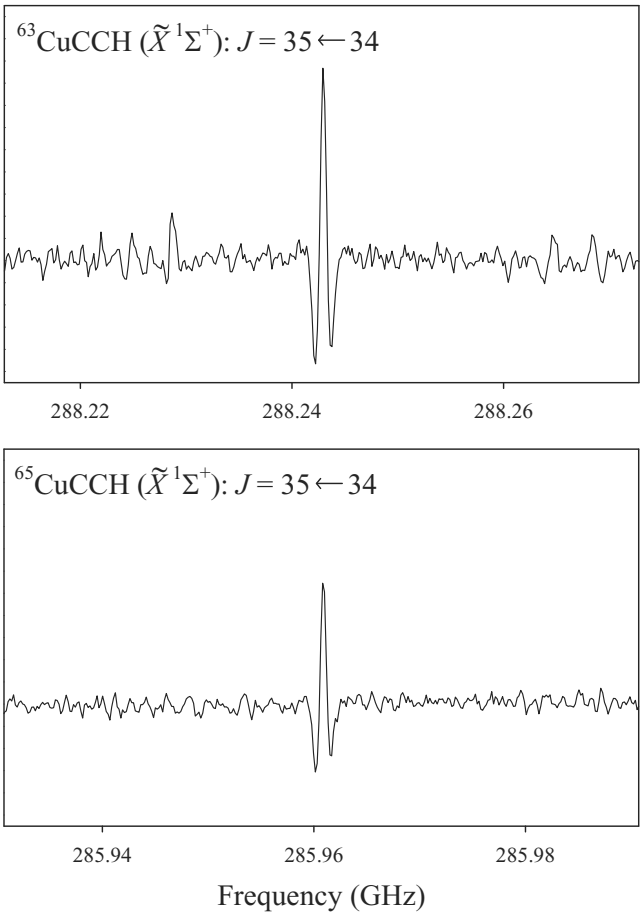

FIG. 4. Millimeter-wave spectra of the $J=35\leftarrow34$ transition of ^{63}CuCCH (upper panel) and ^{65}CuCCH (lower panel) near 288 and 286 GHz, respectively. The quadrupole splittings are sufficiently collapsed at these frequencies that the rotational transitions appear as single lines. The data for ^{63}CuCCH is a single, 110 MHz wide scan acquired in 70 s and cropped to display a 60 MHz wide frequency range; the ^{65}CuCCH spectrum is an average of four such scans. The data are plotted on the same intensity scale to illustrate the ^{63}Cu:^{65}Cu natural abundance ratio.

previously described by Bizzocchi *et al.*[35] These authors used a laser ablation/dc discharge source to create SnTe and SnSe. Bizzocchi *et al.*[35] did not report a dramatic increase in molecule production, but rather an improvement in the population of vibrationally excited states of their molecules when the discharge was applied. They used composite rods to produce the molecules; their discharge nozzle contained an after-flow channel or "integration zone;" and they utilized the 1064 nm laser output with a higher power of 500 mJ/pulse. These are all rather different from our DALAS arrangement. Whether these or other differences in source design are important is yet to be established. As noted by Walker and Gerry,[36] laser ablation in FTMW spectrometers is subject to a wide range of variables that can adversely affect molecule production.

B. Structure and bonding of CuCCH

Molecular r_0, r_s, $r_m^{(1)}$, and $r_m^{(2)}$ structures for CuCCH have been determined from the rotational constants established for the six isotopologues. The r_0 bond lengths were obtained directly from a least-squares fit to the moments of

TABLE II. Spectroscopic constants (MHz) for CuCCH($\tilde{X}\ ^1\Sigma^+$).[a]

Parameter	^{63}CuCCH MW, MMW	Theor.[b]	^{65}CuCCH MW, MMW	^{63}CuC^{13}CH MW	^{63}Cu^{13}CCH MW	^{63}Cu^{13}C^{13}CH MW	^{63}CuCCD MW
B	4120.788 53(65)	4076.34	4088.142 19(68)	3948.3564(13)	4080.0547(18)	3912.6467(18)	3771.034 72(98)
D	0.001 238 56(48)		0.001 220 33(48)	0.001 162(33)	0.001 238(69)	0.001 114(69)	0.000 975(27)
C_l (Cu)	0.0090(18)		0.0091(26)	0.0088(25)	0.0089(27)	0.0085(27)	0.0081(16)
eQq (Cu)	16.391(21)	−12.65	15.169(29)	16.392(29)	16.409(29)	16.408(29)	16.394(19)
eQq (D)							0.214(23)
rms	0.004		0.012	0.002	0.002	0.002	0.002

[a]Errors are 3σ in the last quoted decimal places.
[b]B3LYP/aug-cc-pVTZ.

inertia, while the r_s substitution structure was calculated using Kraitchman's equations, which accounts, in part, for the zero-point vibrational effects.[31] The $r_m^{(1)}$ and $r_m^{(2)}$ geometries were derived by a mass-dependent method developed by Watson.[37] The $r_m^{(2)}$ bond lengths are believed to be closest to the equilibrium structure, as long as isotopic substitution is carried out for every single atom in the molecule, as is the case here. The resulting bond lengths of CuCCH are listed in Table III. As the table shows, depending on the method, the Cu—C bond length is 1.818–1.822 Å, the C—C bond length lies in the range of 1.212–1.217 Å, and the C—H bond length is 1.046–1.058 Å. The r_0, r_s, and $r_m^{(1)}$ structures calculated for CuCCH all agree to within 0.2%, whereas the $r_m^{(2)}$ structure shows a significant difference for the C—H bond of 0.012 Å, which is not surprising considering the deuterium substitution. The r_e structure of CuCCH calculated using the B3LYP method, as described earlier, is given in Table III as well. The theoretical bond distances are all within 1.5% of the $r_m^{(2)}$ structure.

Table III also displays bond lengths of related molecules.[38–40] As can be seen from the table, the C—C and C—H bond lengths for CuCCH are very similar to those in acetylene (HC≡CH). In CuCCH, $r_m^{(2)}$(C—C) = 1.2174(6) Å and $r_m^{(2)}$(C—H) = 1.046(2) Å; for HCCH, r_e(C—C) = 1.20241(9) Å and r_e(C—H) = 1.0625(1) Å.[40] However, it is notable that in the copper compound, the C—C triple bond is slightly longer, while the C—H bond is shorter. The $r_m^{(2)}$ Cu—C bond length [1.8177(6) Å] in CuCCH is slightly shorter than those of CuCN [1.829 62(4) Å] and $CuCH_3$ [1.8809(2) Å].[37,39] Both CuCN and $CuCH_3$ are thought to have single copper-carbon bonds. Given these comparisons, the likely structure of CuCCH is Cu—C≡C—H.

For transition metal complexes with σ-donor ligands such as cyanides, alkenes, alkynes, and alkyls, there is a significant amount of covalent character in the metal-carbon bond. This property probably accounts for the small variations in Cu—C bond lengths among CuCCH, CuCN, and $CuCH_3$. In the covalent scheme, the type of hybridization results in different carbon radii: 0.76 Å for sp^3 and 0.69 Å for sp.[41] When the appropriate carbon radii are subtracted from the Cu—C bond lengths in Table IV, copper covalent radii of 1.13 Å for CuCCH, 1.14 Å for CuCN, and 1.12 Å for $CuCH_3$ are obtained. These values match the Cu(I) covalent radius of 1.17 Å very well.[42] Therefore, the small differences in Cu—C bond lengths in these species reflect the hybridization state of the carbon atom.

C. Interpretation of the hyperfine constants

The magnitude of the experimental electric quadrupole coupling constant, $eQq(^{63}\text{Cu}) = +16.391(21)$ MHz, is similar

TABLE III. Bond lengths of CuCCH and related species.[a]

Molecule	r(M–C) (Å)	r(C—C) (Å)	r(C—H) (Å)	Method	Ref.
CuCCH($\tilde{X}\ ^1\Sigma^+$)	1.818(1)	1.212(2)	1.058(1)	r_0	This work
	1.819	1.213	1.058	r_s	This work
	1.822(1)	1.213(2)	1.058(1)	$r_m^{(1)}$	This work[b]
	1.8177(6)	1.2174(6)	1.046(2)	$r_m^{(2)}$	This work[c]
	1.834	1.212	1.062	r_e, B3LYP	This work
CuCN($\tilde{X}\ ^1\Sigma^+$)	1.832 31(7)			r_0	38
	1.832 84(4)			r_s	38
	1.829 62(4)			$r_m^{(2)}$	38
$CuCH_3$($\tilde{X}\ ^1A_1$)	1.8841(2)		1.091(2)	r_0	39
	1.8817(2)		1.0923(2)	r_s	39
	1.8799(2)		1.0914(3)	$r_m^{(1)}$	39
	1.8809(2)		1.0851(1)	$r_m^{(2)}$	39
HC≡CH		1.202 41(9)	1.0625(1)	r_e, infrared, Raman	40

[a]Values in parentheses are 1σ uncertainties.
[b]$c_b = -0.028(8)$.
[c]$c_b = -0.091(3)$ and $d_b = 0.401(18)$.

TABLE IV. Copper eQq values of CuCCH and other related species.

Species	eQq or χ_{aa} (MHz)	Ref.
CuCN	24.523(17)	45
CuF	21.9562(24)	43
CuCCH	16.391(21)	This work
CuCl	16.16908(72)	44
CuOH	10.572(49)	45
CuSH	5.642(49)	45
$CuCH_3$	−3.797(49)	45

to the theoretical value, but is opposite in sign. An analysis using a negative value of eQq for CuCCH did not produce a reasonable fit (rms value of several MHz), and the strengths of the predicted transitions did not reproduce the observed intensities of the FTMW data. A positive value of eQq for Cu has been established for most other copper-containing species, such as CuF, CuCl, CuBr, and CuCN.[43–45] The ratio $eQq(^{63}\text{CuCCH})/eQq(^{65}\text{CuCCH}) \sim 1.082$ is in excellent agreement with the ratio of quadrupole moments of the respective atoms (1.082) with $Q(^{63}\text{Cu}) = -0.211$ barns (1 barn $= 10^{-24}$ cm^2) and $Q(^{65}\text{Cu}) = -0.195$ barns.[46]

The ^{63}Cu electric quadrupole coupling constants (eQq for linear molecules and χ_{aa} for nonlinear species) for related copper-containing species are listed in Table IV.[43–45] These numbers range from +24.5 MHz in CuCN to −3.8 MHz in $CuCH_3$.[45] As seen in the table, CuCCH and CuCl have a similar eQq value of ~16 MHz, as do CuF and CuCN (~24 MHz). The values of eQq are smaller for CuOH and CuSH, while that in $CuCH_3$ is negative. Relating the degree of ionic character of the halides CuF and CuCl to the eQq constants suggest simplistically that CuCN is quite ionic, as is CuCCH, while CuOH, CuSH, and $CuCH_3$ are mostly covalent. However, the CuCCH structure suggests a large degree of covalent character. Moreover, if CuCN were very ionic, it should have a T-shaped structure similar to NaCN and KCN.[47,48] As explained by Gerry and co-worker,[43] the analysis of copper quadrupole constants often does not present a coherent picture.

Perhaps a clearer approach would be to employ the modified Townes–Dailey model to calculate the Cu quadrupole constants,[49] using the relationship[43]

$$eQq = eQq_{410}\left(n_{4p\sigma} - \frac{1}{2}n_{4p\pi}\right) + eQq_{320}\left(n_{3d\sigma} + \frac{1}{2}n_{3d\pi} - n_{3d\delta}\right). \quad (2)$$

Here eQq_{410} and eQq_{320} are the copper quadrupole coupling constants containing singly occupied $4p\sigma$ and $3d\sigma$ atomic orbitals, 31.19 and 231.22 MHz,[43] respectively, and the n's are the valence molecular orbital populations. Since Cu has a filled $3d$ subshell, the second term is zero to a first approximation. As demonstrated earlier, the carbon atom in the Cu—C bond is sp hybridized, so one might assume there is some degree of $4s$-$4p$ hybridization for the copper atom. In the simplest picture, the amount of $4p\sigma$ character would be 0.5, with no $4p\pi$ character. Using these assumptions, the eQq for CuCCH is calculated to be 15.6 MHz. This quantity agrees well with the experimental value of 16.391(21) MHz. This approach could also be applied to CuCN, for which the experimental ^{63}Cu eQq parameter is 24.523(17) MHz, about 40% larger than the calculated value of 15.6 MHz. Previously, Gerry and co-worker[43] attempted to apply the modified Townes–Dailey model to CuF and CuCl, but without much success. They concluded that the model could not "cope" with copper coupling constants.

Copper is a transition metal and has $3d$ electrons. In the case of CuCCH and CuCN, the ligands have triple bonds and empty π^* orbitals, allowing backbonding from the $3d$ electrons of copper. This backbonding could easily affect the orbital populations and alter the inferred eQq values from Eq. (2). Therefore, a simple comparison with CuF and CuCl may not be realistic. Furthermore, in the case of $CuCH_3$, the eQq value is small and negative, and changes sign with respect to the other copper compounds. In this case, there are no empty π^* orbitals, and no backbonding to the methyl ligand, likely causing a quite different charge distribution around the Cu nucleus.

In CuCCD, the deuterium quadrupole coupling is much smaller in comparison to that of copper: 0.214(23) MHz versus 16.391(21) MHz. Within the uncertainties, this difference appears to reflect the variation in quadrupole moments of the respective nuclei: 0.0028 barns versus −0.211 barns.[46] However, it is certain that the electric field distribution at the deuterium nucleus dramatically differs from that of copper. It is noteworthy that the sign of Q changes for the deuterium nucleus relative to copper, but both eQq values have the same sign.

VI. CONCLUSION

CuCCH, which is a model system for larger CuCCR species, has now been characterized in the gas phase. Analysis of its molecular structure suggests a Cu—C single bond with an acetylenic ligand. A comparison of the Cu quadrupole coupling constants of CuCCH with other copper species suggests that a more complex interpretation is needed where transition metals are concerned, especially if backbonding is involved. This work also has demonstrated the viability of a new synthetic technique, DALAS, which couples laser ablation with a dc discharge. This method has potential for the study of other transition metal species of interest to synthetic chemistry and catalysis. Finally, this work shows the versatility gained by combining FTMW spectroscopy with millimeter-wave techniques.

ACKNOWLEDGMENTS

This research is supported by NSF Grant No. CHE 07-18699. D.J.C. also thanks the NSF for support and the Ziurys group for their hospitality during his sabbatical leave.

[1] *Modern Organocopper Chemistry*, edited by N. Krause (Wiley-VCH, Weinheim, 2002).
[2] M. S. Kharasch and P. O. Tawney, J. Am. Chem. Soc. **63**, 2308 (1941).
[3] J. F. Normant, Synthesis **1972**, 63 (1972).
[4] H. Gilman, R. G. Jones, and L. A. Woods, J. Org. Chem. **17**, 1630 (1952).
[5] F. Ullmann and J. Bielecki, Chem. Ber. **34**, 2174 (1901).
[6] J. Hassan, M. Sévignon, C. Gozzi, E. Schulz, and M. Lemaire, Chem.

Rev. (Washington, D.C.) **102**, 1359 (2002).
[7] R. C. Böttger, Justus Liebigs Annalen der Chemie **109**, 351 (1859).
[8] K. Judai, J. Nishijo, and N. Nishi, Adv. Mater. (Weinheim, Ger.) **18**, 2842 (2006).
[9] R. D. Stephens and C. E. Castro, J. Org. Chem. **28**, 3313 (1963).
[10] C. E. Castro, R. Havlin, V. K. Honwad, A. Malte, and S. Moje, J. Am. Chem. Soc. **91**, 6464 (1969).
[11] W. Chodkiewicz, Ann. Chim. (Paris) **2**, 819 (1957).
[12] P. Cadiot and W. Chodkiewicz, in *Chemistry of Acetylenes*, edited by H. G. Viehe (Dekker, New York, 1969), p. 597.
[13] K. Sonogashira, Y. Tohda, and N. Hagihara, Tetrahedron Lett. **16**, 4467 (1975).
[14] C. S. Xie, L. F. Liu, Y. H. Zhang, and P. X. Xu, Org. Lett. **10**, 2393 (2008).
[15] M. Eckhardt and G. C. Fu, J. Am. Chem. Soc. **125**, 13642 (2003).
[16] V. Calo, L. Lopez, G. Marchese, and G. Pesce, Tetrahedron Lett. **20**, 3873 (1979).
[17] T. N. Jin, S. Kamijo, and Y. Yamamoto, Eur. J. Org. Chem. 3789 (2004).
[18] P. Bertus, F. Fecourt, C. Bauder, and P. Pale, New J. Chem. **28**, 12 (2004).
[19] R. Chinchilla and C. Nájera, Chem. Rev. (Washington, D.C.) **107**, 874 (2007).
[20] F. Cataldo and D. Capitani, Mater. Chem. Phys. **59**, 225 (1999).
[21] T. Aleksanyan, I. A. Garbuzova, I. R. Gol'ding, and A. M. Sladkov, Spectrochim. Acta, Part A **31**, 517 (1975).
[22] M. J. Frisch, G. W. Trucks, H. B. Schlegel *et al.*, GAUSSIAN 03, Revision C.02, Gaussian, Inc., Wallingford, CT, 2004.
[23] A. D. Becke, J. Chem. Phys. **98**, 5648 (1993).
[24] C. Lee, W. Yang, and R. G. Parr, Phys. Rev. B **37**, 785 (1988).
[25] T. H. Dunning, Jr., J. Chem. Phys. **90**, 1007 (1989).
[26] T. J. Balle and W. H. Flygare, Rev. Sci. Instrum. **52**, 33 (1981).
[27] M. Sun, A. J. Apponi, and L. M. Ziurys, J. Chem. Phys. **130**, 034309 (2009).
[28] L. M. Ziurys, W. L. Barclay, Jr., M. A. Anderson, D. A. Fletcher, and J. W. Lamb, Rev. Sci. Instrum. **65**, 1517 (1994).
[29] C. H. Townes and A. L. Schawlow, *Microwave Spectrosc* (Dover, New York, 1975).
[30] See supplementary material at http://dx.doi.org/10.1063/1.3493690 for a complete list of the measured transition frequencies of CuCCD.
[31] W. Gordy and R. L. Cook, *Microwave Molecular Spectra* (Wiley, New York, 1984).
[32] H. M. Pickett, J. Mol. Spectrosc. **148**, 371 (1991).
[33] G. V. Chertihin and L. Andrews, J. Chem. Phys. **106**, 3457 (1997).
[34] M. A. Blitz, S. A. Mitchell, and P. A. Hackett, J. Phys. Chem. **95**, 8719 (1991).
[35] L. Bizzocchi, B. M. Giuliano, M. Hess, and J. U. Grabow, J. Chem. Phys. **126**, 114305 (2007).
[36] K. A. Walker and M. C. L. Gerry, J. Mol. Spectrosc. **182**, 178 (1997).
[37] J. K. G. Watson, A. Roytburg, and W. Ulrich, J. Mol. Spectrosc. **196**, 102 (1999).
[38] D. B. Grotjahn, M. A. Brewster, and L. M. Ziurys, J. Am. Chem. Soc. **124**, 5895 (2002).
[39] D. B. Grotjahn, D. T. Halfen, L. M. Ziurys, and A. L. Cooksy, J. Am. Chem. Soc. **126**, 12621 (2004).
[40] E. Kostyk and H. L. Welsh, Can. J. Phys. **58**, 912 (1980).
[41] B. Cordero, V. Gómez, A. E. Platero-Prats, M. Revés, J. Echeverría, E. Cremades, F. Barragán, and S. Alvarez, Dalton Trans. 2832 (2008).
[42] P. Pyykkö, Chem. Rev. (Washington, D.C.) **88**, 563 (1988).
[43] C. J. Evans and M. C. L. Gerry, J. Chem. Phys. **112**, 9363 (2000).
[44] R. J. Low, T. D. Varberg, J. P. Connelly, A. R. Auty, B. J. Howard, and J. M. Brown, J. Mol. Spectrosc. **161**, 499 (1993).
[45] M. Sun, D. T. Halfen, D. J. Clouthier, and L. M. Ziurys (unpublished).
[46] N. J. Stone, At. Data Nucl. Data Tables **90**, 75 (2005).
[47] J. J. van Vaals, W. L. Meerts, and A. Dymanus, Chem. Phys. **86**, 147 (1984).
[48] T. Törring, J. P. Bekooy, W. L. Meerts, J. Hoeft, E. Tiemann, and A. Dymanus, J. Chem. Phys. **73**, 4875 (1980).
[49] C. H. Townes and B. P. Dailey, J. Chem. Phys. **17**, 782 (1949).